

Suzaku Reveals Helium-burning Products in the X-ray Emitting Planetary Nebula BD +30° 3639

M. Murashima¹, M. Kokubun¹, K. Makishima^{1,2}, J. Kotoku³, H. Murakami⁴,
K. Matsushita⁵, K. Hayashida⁶, K. Arnaud⁷, K. Hamaguchi⁷, and H. Matsumoto⁸

1: *Department of Physics, University of Tokyo, 7-3-1 Hongo, Bunkyo-ku, Tokyo 113-0011,
Japan*

2: *The Institute of Physical and Chemical Research, 2-1 Hirosawa, Wako, Saitama
351-0198, Japan*

3: *Department of Physics, Tokyo Institute of Technology, O-okayama, Meguro-ku, Tokyo
152-8551, Japan*

4: *PLAIN Center, ISAS/JAXA, 3-1-1 Yoshinodai, Sagami-hara, Kanagawa 229-8510, Japan*

5: *Department of Physics, Tokyo University of Science, Kagurazaka, Shinjuku-ku, Tokyo
162-8601, Japan*

6: *Department of Space and Earth Science, Osaka University, Toyonaka, Osaka 560-0043,
Japan*

7: *Exploration of the Universe Division, Code 660, NASA/GSFC, Greenbelt, MD 20771,
USA*

8: *Department of Physics, Kyoto University, Kitashirakawa, Sakyo-ku, Kyoto 606-8502,
Japan*

ABSTRACT

BD +30° 3639, the brightest planetary nebula at X-ray energies, was observed with *Suzaku*, an X-ray observatory launched on 2005 July 10. Using the X-ray Imaging Spectrometer, the K-lines from C VI, O VII, and O VIII were resolved for the first time, and C/O, N/O, and Ne/O abundance ratios determined. The C/O and Ne/O abundance ratios exceed the solar value by a factor of at least 30 and 5, respectively. These results indicate that the X-rays are emitted mainly by helium shell-burning products.

Subject headings: planetary nebulae: general — planetary nebulae: individual(BD +30° 3639), X-ray

1. Introduction

Intermediate-mass stars, with initial masses $\lesssim 8 M_{\odot}$, are thought to contribute significantly to the synthesis of C, N, O, and Ne through the CNO cycle and He burning. These nuclear fusion products are ejected through mass loss as the stars evolve from their AGB (asymptotic giant branch) phase into planetary nebulae (PNe). Hence, a PN can be regarded as a messenger bearing information on the nucleosynthesis within these stars. However, the optically-visible material in PNe represents matter accumulated over the PN lifetime, making it difficult to extract information on, for instance, pure He-burning products just by observing the PNe shells.

Soft X-rays, detected from several PNe, are thought to originate in hot plasmas produced by shocks in fast stellar winds (Kwok 1982; Volk & Kwok. 1985). These fast winds develop during the later evolutionary stages of the central star, so the X-rays are thought to be emitted by the star’s late-phase products. X-ray spectroscopy of PNe will thus allow us to diagnose products of a particular nucleosynthesis phase inside intermediate-mass stars. However, it has been difficult to resolve K-lines from C, N, and O, the major CNO and He-burning products, because the line energies were too low for X-ray CCDs. In addition, these objects are often too X-ray faint for high-resolution spectroscopy using gratings, even when their angular size is small enough.

The 5th Japanese X-ray satellite *Suzaku* (*Astro-E2*; Mitsuda et al. 2004) was developed by a Japan-US collaboration as a successor to *ASCA*, and was launched successfully on 2005 July 10. Its X-ray Imaging Spectrometer (XIS) comprises four CCD cameras, XIS-0 through XIS-3 (Hayashida et al. 2004). Three of the cameras use front-illuminated (FI) CCD chips while XIS-1 utilizes the back-illuminated (BI) technology. Compared to similar instruments on preceding X-ray missions, both the BI and FI chips have better responses to X-rays with energies below ~ 1 keV: their FWHM energy resolution at 0.5 keV is ~ 40 eV (FI) and ~ 50 eV (BI), with insignificant low-energy tails.

We observed the PN, BD +30° 3639, with *Suzaku* in order to resolve the anticipated carbon and oxygen emission lines. Since its detection using *ROSAT* (Kreysing et al. 1992), this object has been known as the X-ray brightest PN, emitting spatially-extended soft X-rays from inside its $\sim 4''$ diameter optical shell (Kastner et al. 2000). The X-ray emitting plasma is thought to have highly non-solar abundance ratios, as shown by the strong Ne-K line first detected using *ASCA* (Arnaud et al. 1996), and a broad sub-keV spectral hump, presumably a blend of C, N, and O lines, subsequently detected with *Chandra* (Kastner et al. 2000; Maness et al. 2003).

2. Observation

The present observation of BD +30° 3639 was performed for a net exposure of 34.4 ksec on 2005 September 20, (seq. no. 100025010), as part of the initial performance verification of *Suzaku*. Both the XIS and the Hard X-ray Detector (HXD; Kawaharada et al. (2004)) onboard were operated in their nominal modes. We do not however use the HXD data, since its non-imaging $34' \times 34'$ field of view also contains part of the large supernova remnant, G65.2+5.7, which overlaps with the target PN.

The target was clearly detected in all XIS cameras; Figure 1 shows 0.3–0.7 keV images obtained with two of them. We define the source region as a $2'.5$ radius circle centered on the source, which encloses $\sim 90\%$ of signal photons from the PN that is essentially a point source at the angular resolution of the *Suzaku* X-ray Telescopes. The background region is defined as a surrounding annulus with an outer radius of $5'$, as indicated in Figure 1a. After background subtraction, net signal counts are 1116 ± 46 , 3039 ± 74 , 1174 ± 47 , and 1012 ± 44 from XIS-0, 1, 2, and 3, respectively. Since the three FI cameras (XIS-0, 2, 3) are essentially identical, we co-add their data, and refer to them as “XIS-023” below.

3. Analysis and Results

As shown in Figure 2, the on-source XIS-1 spectrum clearly reveals at 0.37 keV the K_α line from hydrogenic carbon (C VI). Its absence in the background spectrum ensures that the line is coming from the PN itself. The spectra also show K_α lines from O VII, O VIII, and Ne IX. Some of these lines are found in the background spectrum as well, but with much reduced intensities; these background lines are thought to come from diffuse Galactic soft X-ray components which may well extend to the present Galactic latitude of $5.^\circ$, possibly with additional contribution from G65.2+5.7.

At a temperature of $kT \sim 0.3$ keV (Arnaud et al. 1996; Maness et al. 2003), the C VI to O VII (the triplet summed) line emissivity ratio of a solar-ratio plasma is ~ 0.15 . As illustrated in Figure 2 in green, this ratio will be reduced to ~ 0.03 (Murashima 2006) due to interstellar plus intra-nebular absorption (with the latter probably dominant; Kastner et al. (2002)), and the decrease in XIS-1 efficiency toward lower energies. Nevertheless, the XIS-1 spectrum yields comparable numbers of C VI and O VII line photons, suggesting a highly enhanced C/O ratio of the X-ray emitting plasma.

This early in the mission, the XIS calibration is still being fine-tuned. There are uncertainties in the energy gain, and also in the low-energy efficiency which has decreased since the start of observations. We solved the former by self-calibrating (within $\sim 3\%$) the

gains using the emission lines from BD +30° 3639 themselves. The latter effect is attributed to excess absorption due to the build-up of contaminant in front of the XIS cameras. We estimated the chemical composition of the excess absorber using a *Suzaku* observation of the isolated neutron star RX J1856.6-3574 (Murashima 2006), which is known to exhibit a blackbody with a temperature of 63 eV, absorbed by a low column of $N_{\text{H}} = 0.087 \times 10^{21} \text{ cm}^{-2}$ (Burwitz et al. 2003). To accurately determine the contaminant thickness for XIS-1 and (separately) XIS-023, we included in all analysis a simultaneous fit to the archival (ObsId 587) background-subtracted *Chandra* ACIS-S spectrum of the same object.

We jointly fit the background-subtracted XIS-1, XIS-023, and *Chandra* ACIS-S spectra, using an absorbed single-temperature vAPEC model (Smith et al. 2001). The abundances (relative to solar; Anders & Gevesse (1989)) of C, N, O, Ne, and Fe, were left free; that of He fixed to solar; other heavy elements were neglected; kT and the intervening (interstellar plus intra-nebular) hydrogen column density N_{H} were left free. As shown in Figure 3, the model gives a reasonable joint fit to the three spectra, with $\chi^2/\nu = 331/228$. We determined $kT = 0.19 \pm 0.01 \text{ keV}$ and $N_{\text{H}} = (2.1_{-0.7}^{+0.4}) \times 10^{21} \text{ cm}^{-2}$. Figure 3 also illustrates the difference in the energy-resolving power between the XIS and ACIS-S.

This fitting procedure cannot in reality constrain the absolute (i.e., relative to hydrogen) metal abundances, since the low-energy flux from a plasma with $kT \sim 0.2 \text{ keV}$ is dominated by emission lines from the metals themselves, even when the metallicity is ~ 1 solar. Furthermore, the continua, due to hydrogen, (presumably non-solar abundance) helium, and the enhanced metals themselves, cannot be independently determined. Nevertheless, we expect abundance *ratios* among metals to be reasonably constrained by the lines which are individually resolved with the XIS. To see this, we produced in Figure 4 confidence contours for the C and O abundances using the joint vAPEC fits. Thus, the contours are highly elongated along the proportionality between the two quantities, and the C/O ratio is successfully constrained as $104 > \text{C/O} > 71$ solar at 90% confidence with the best estimate at 85. (The range does not change significantly even allowing N_{H} to float.) In the same way, we have obtained $5.5 > \text{N/O} > 0.9$ and $7.5 > \text{Ne/O} > 4.7$, with the best fits of 3.2 and 5.8, respectively, and $\text{Fe/O} < 0.1$, all in solar units. Below, these results are examined for various systematic effects.

We have so far assumed the He/H ratio to be solar. However, increasing it to 5, 10, or 20 solar does not affect the relative C/N/O/Ne abundances by more than 5%. Similarly, the results remain unchanged within $\sim 10\%$ when the thickness of the XIS excess absorber is varied by $\pm 20\%$ around the best estimates (equivalent to $N_{\text{H}} \sim 8 \times 10^{20} \text{ cm}^{-2}$), or the background spectra are derived from several other regions (e.g., using larger annuli or using limited azimuthal sectors) in the XIS field of view.

To relax the assumption of isothermality, we refitted the three spectra jointly with a sum of two vAPEC components, which are constrained to share common abundances and the same N_{H} . We tentatively fixed the C/O ratio at various trial values, and let the two temperatures vary freely. Even with this extra degree of freedom, acceptable fits were reproduced only when the assumed C/O ratio is in the range 35–120 solar. The two temperatures were typically found at ~ 0.12 keV and ~ 0.22 keV. Further, the C/O ratio stayed above ~ 30 even when fitted with a model allowing non-equilibrium ionization conditions.

The largest systematic effect on our results comes from uncertainty in N_{H} , because our best-fit value ($N_{\text{H}} \sim 2 \times 10^{21} \text{ cm}^{-2}$) is twice that estimated from extinction data at longer wavelengths (Cahn et al. 1992; Arnaud et al. 1996; Kastner et al. 2000). We therefore repeated the joint, single-vAPEC fit to the three spectra, but this time fixing N_{H} at $1 \times 10^{21} \text{ cm}^{-2}$. Then, kT increased to ~ 0.23 keV, and the C/O ratio decreased by a factor of ~ 3 , while the Ne/O ratio remained nearly unchanged. These new parameters are consistent with the recent *Chandra* LETG results on BD +30° 3639 (Kastner et al. 2006). However, the (non-reduced) χ^2 for the joint fit to the *Suzaku* XIS and *Chandra* ACIS data increases by ~ 25 when N_{H} is forced to take the smaller value. This suggests that the X-ray absorption is actually higher than is implied by the extinction data, perhaps because the intra-nebular absorber is metal-enriched.

Based on these evaluations, we take as our result the original single-vAPEC solution (i.e., C/O ~ 85) with free N_{H} , with the reservation that the C/O ratio could be subject to a systematic over-estimation by a factor of ~ 3 . This factor reflects possible non-isothermality, non-equilibrium ionization conditions, or the uncertainty in N_{H} . In any event, the very high carbon over-abundance relative to oxygen is a robust result, confirming the previous suggestions (Arnaud et al. 1996; Kastner et al. 2000; Maness et al. 2003).

4. Discussion

The three spectra analyzed consistently indicate an absorbed 0.2–2.0 keV flux of $6.5 \times 10^{-12} \text{ erg s}^{-1}$, in agreement with previous measurements (Maness et al. 2003). Correction for the absorption by $N_{\text{H}} = 2 \times 10^{21} \text{ cm}^{-2}$ increases this flux by a factor of ~ 9 , yielding an absorption-corrected 0.2–2.0 keV luminosity of $\sim 1.4 \times 10^{33} \text{ ergs s}^{-1}$ at a distance of 1.3 kpc (Mellema 2004). (If the fit with $N_{\text{H}} = 1 \times 10^{21} \text{ cm}^{-2}$ is used, the absorption-corrected quantities become smaller than these by a factor of ~ 3 .) This is only $\sim 0.1\%$ of the kinetic luminosity, $\sim 1.2 \times 10^{36} \text{ ergs s}^{-1}$, supplied by the fast stellar wind (de Freitas Pacheco et al. 1993). This, together with the X-ray emitting region just fitting inside the optical shell (Kastner et al. 2000), supports the interacting wind model (Kwok 1982; Volk & Kwok. 1985)

as a scenario to explain the X-ray emission from this PN.

Observations in the optical and neighboring wavelengths give the nebular abundance ratios of BD +30° 3639 as C/O \sim 3.7, N/O \sim 1.8, and Ne/O \sim 2.8 in solar units (Bernard-Salas et al. 2003). Compared with these, our X-ray results imply qualitatively similar, but much more extreme, abundance patterns. This is not surprising, since the X-ray emitting plasma is considered to represent a very limited radial zone of the stellar interior. In fact, assuming, based on the *Chandra* image, that the X-ray emitting plasma fills a sphere of radius 0.01 pc (1".6), its mass is estimated as $\sim 5 \times 10^{-4} M_{\odot}$ from the observed emission measure of $5.7 \times 10^{55} \text{ cm}^{-3}$. This can be supplied only in ~ 70 yr by the mass loss of $\sim 7 \times 10^{-6} M_{\odot} \text{ yr}^{-1}$ from the central star (de Freitas Pacheco et al. 1993).

Which part of the stellar interior provides the X-ray emitting plasma? The most outstanding feature is the extreme carbon enhancement over oxygen, by a factor of ~ 40 in the *number* ratio, or ~ 30 in the *mass* ratio. This is a typical value expected from competition between the triple- α and $^{12}\text{C}(\alpha, \gamma)^{16}\text{O}$ reactions during He shell-burning flashes (Herwig 2005; Suda et al. 2004), for an initial mass of $\sim 2 M_{\odot}$. Therefore, we presume that the X-rays come primarily from products of He shell-burning episodes which took place in the AGB phase. The possible factor-of-three uncertainty will not affect this inference significantly, since the theoretical calculations are thought to be uncertain to a similar degree.

The observed high Ne/O ratio, in contrast, requires a neon-producing path without ^{16}O . Presumably ^{14}N , concentrated through the CNO cycle, burnt as $^{14}\text{N}(\alpha, \gamma)^{18}\text{F}(\beta^+, \nu)^{18}\text{O}(\alpha, \gamma)^{22}\text{Ne}$ during the He shell flashes. This produces ^{22}Ne , which is indistinguishable in X-rays from the more abundant ^{20}Ne . Finally, the hint of enhanced N/O ratio can be explained if some fraction of the nitrogen from the CNO cycle, stored in the upper He layer, escaped without being caught up in the He shell burning.

These considerations lead us to the following scenario for this PN. The hydrogen-rich envelope is likely to have already been expelled. The outer parts of the He layer, composed of radiative and convective zones, are currently being ejected in the form of fast stellar winds with a velocity of $\sim 1000 \text{ km s}^{-1}$. The winds carry the abundant carbon and ^{22}Ne produced in He shell flashes (Herwig 2005), as well as unprocessed nitrogen. These ejecta are shock-heated to emit X-rays.

A more quantitative comparison with the optical spectra of the central stars of PNe (Leuenhagen & Hamann 1998) will provide a valuable calibration of the models of stellar evolution and nucleosynthesis. Such work may also allow us to estimate the initial progenitor mass, and to clarify when the fast stellar winds start blowing. In closing, the present *Suzaku* observation has provided a valuable opportunity of witnessing the carbon nucleosynthesis

inside an evolved star, which is one of the central building blocks of the modern astronomy but has rarely been observed directly.

MM, together with the co-authors, expresses her deepest gratitude to the *ASTRO-E/Astro-E2/Suzaku* project members. Authors thank Prof. Masayuki Fujimoto and Dr. Takuma Suda of Hokkaido University for elucidating discussion. They are also grateful to Dr. Joel Kastner of Rochester Institute of Technology for communicating their latest *Chandra* LETG results on BD +30° 3639.

Facilities: Suzaku (XIS).

REFERENCES

- Anders, E. & Grevesse, N. 1989, *Geochem. Cosmochem. Acta*, 53, 197
- Arnaud, K., Borkowski, K. J., & Harrington, J. P. 1996, *ApJ*, 462, 75
- Bernard-Salas, J., Pottasch, S. R., Wesselius, P. R., & Feibelman, W. A. 2003, *A&A*, 406, 165
- Burwitz, V., Harbel, F., Neuhäuser, R., Predehl, P., Trümper, J., & Zavlin, V. E. 2003, *A&A*, 399, 1109
- Cahn, J., Kaler, J., & Stanghellini, L. 1992, *A&AS*, 94, 399
- de Freitas Pacheco, J. A., Costa, R. D. D., de Araujo, F. X., & Petrini, D. 1993, *MNRAS*, 260, 401
- Hayashida, K., et al. 2004, *SPIE*, 5488, 73
- Herwig, F. 2005, *ARA&A*, 43, 435
- Kastner, J. H., Soker, N., Vrtilik, S. D., & Dgani, R. 2000, *ApJ*, 545, 57
- Kastner, J. H., Li, J., Vrtilik, S., Gatley, I., Merrill, K. M., & Soker, N. 2002, *ApJ*, 581, 1225
- Kastner, J. H., Yu, Y. S., Houck, H., Behar, E., Nordon, R., & Soker, N. 2006, *Proc. IAU Symp.* 234, eds. R. Mendez et al., in press
- Kawaharada, M. et al. 2004, *SPIE*, 5501, 286

- Kreysing, H. C., Diesch, C., Zweigle, J., Staubert, R., Grewing, M., & Hasinger, G. 1992, A&A, 264, 623
- Kwok, S. 1982, ApJ, 258, 280
- Leuenhagen, U., & Hamann, W.-R. 1998, A&A, 330, L265
- Maness, H. L., Vrtilik, S. D., Kastner, J. H., & Soker, N. 2003, ApJ, 589, 439
- Mellema, G. 2004, A&A, 416, 623
- Mitsuda, K., Kunieda, H., Inoue, H., & Kelley, R. 2004, SPIE, 5488, 177
- Murashima, M. 2006, PhD Thesis, the University of Tokyo
- Smith, R. K., Brickhouse, N. S., Liedahl, D. A., & Raymond, J. C. 2001, ApJ, 556, L91
- Suda, T., Aikawa, M., Machida, M. N., Fujimoto, M. Y., & Iben, I. J. 2004, ApJ, 611, 476
- Volk, K., & Kwok, S. 1985, A&A, 153, 79

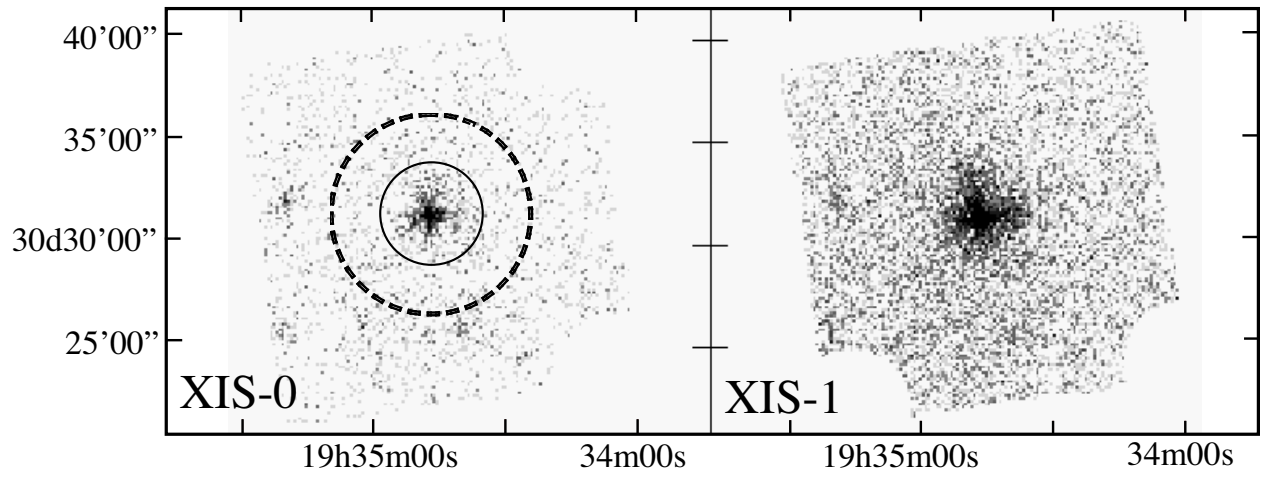


Fig. 1.— Images of BD +30° 3639 in 0.3–0.7 keV, taken with XIS-0 (FI-CCD; left) and XIS-1 (BI-CCD; right). Two circles specify on-source and background data accumulation regions.

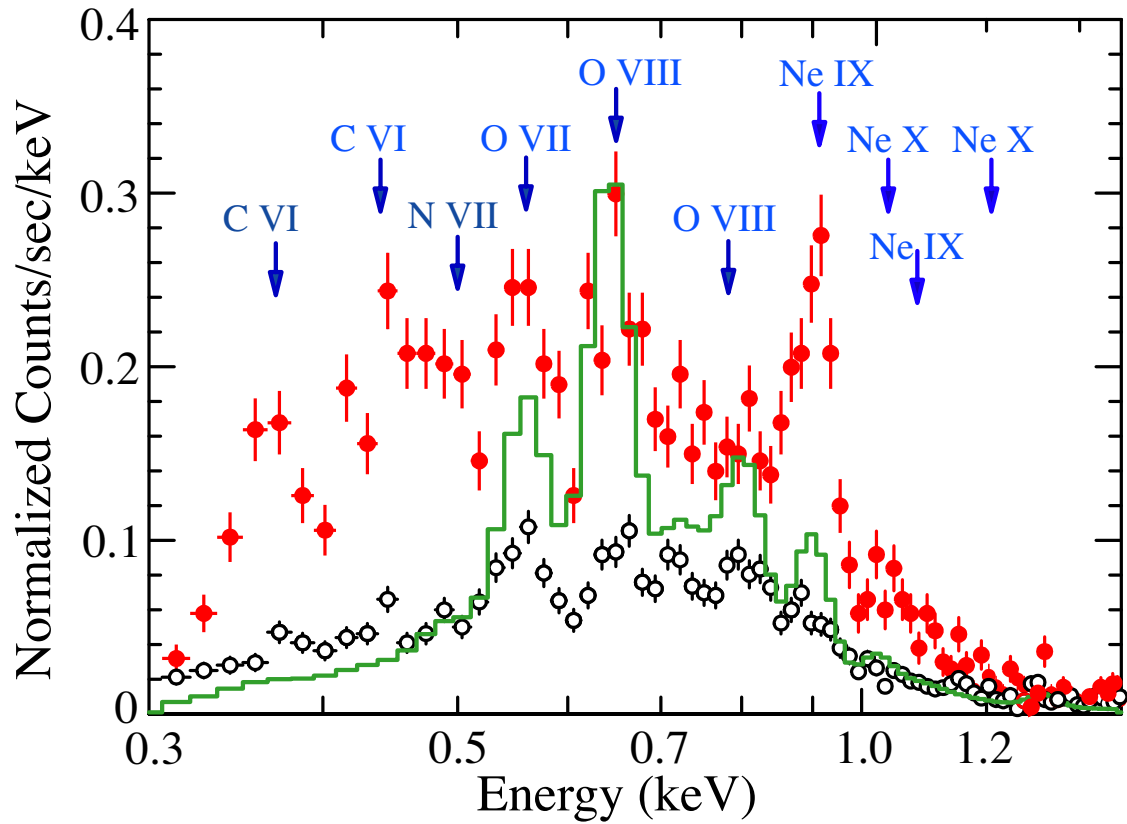


Fig. 2.— Spectra obtained with XIS-1 (BI). Red filled circles show the on-source (background inclusive) data, and black open circles the background. The prediction of an absorbed 1-solar abundance model with $kT = 0.2$ keV is sketched in green. Positions of major lines are indicated in blue.

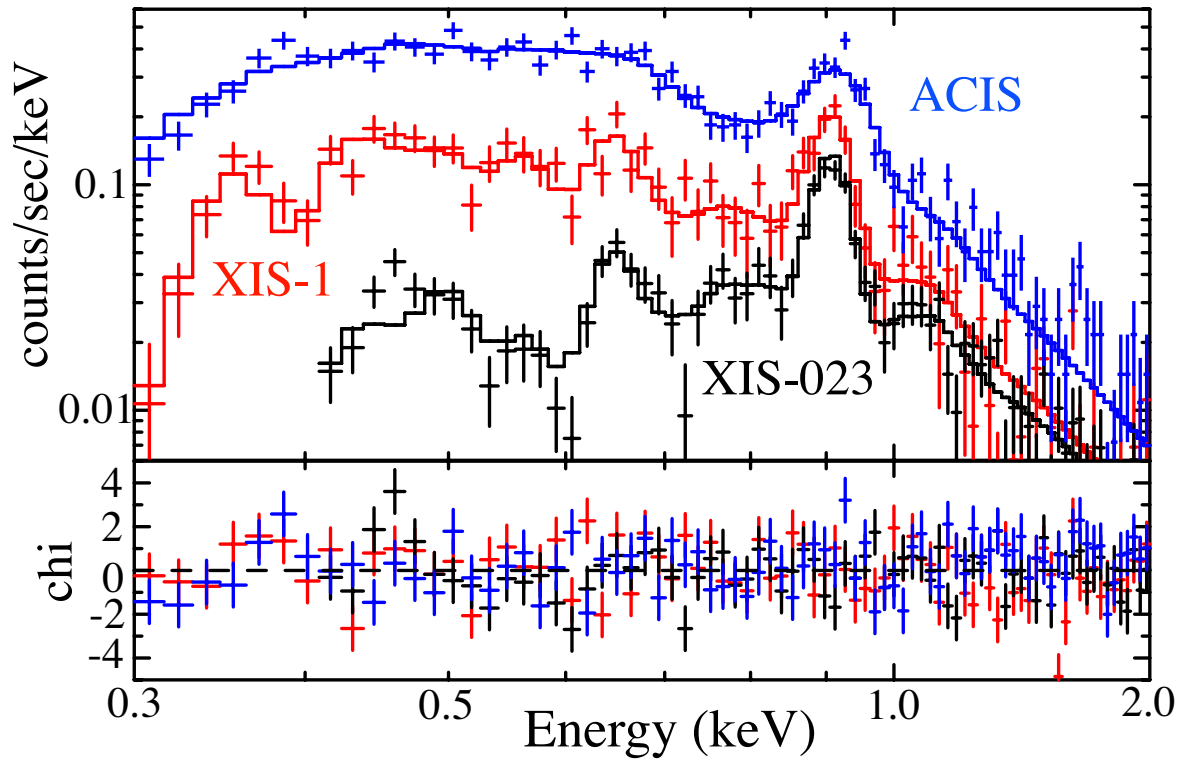


Fig. 3.— Background-subtracted XIS-1 (red), XIS-023 (black), and *Chandra* ACIS-S (blue) spectra of BD +30° 3639, fitted jointly by an absorbed vAPEC model. The XIS responses take into account the excess absorption.

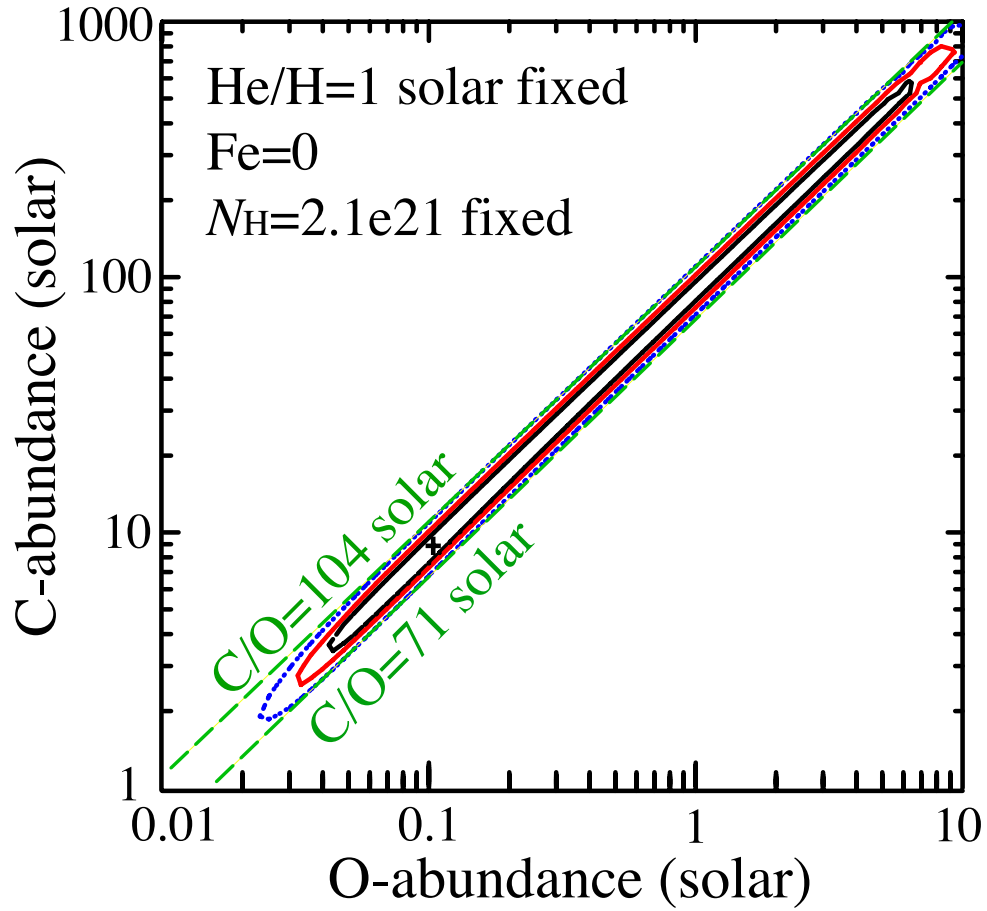


Fig. 4.— Confidence contours for the O and C abundances, derived from the single vAPEC fit of Figure 3. The 69% (black solid), 90% (red solid), and 99% (blue dotted) confidence contours are drawn. The other parameters are left free, except for those described in the figure.